ELSEVIER

Journal of Alloys and Compounds 408–412 (2006) 820–823

Journal of ALLOYS AND COMPOUNDS

www.elsevier.com/locate/jallcom

Glycothermal synthesis and photoluminescence of YAG:Ce^{3+} nanophosphors

R. Kasuya [a], T. Isobe [a,*], H. Kuma [b]

[a] *Faculty of Science and Technology, Keio University, 3-14-1 Hiyoshi, Kohoku-ku, Yokohama 223-8522, Japan*

[b] *Idemitsu Kosan Co. Ltd., 1280, Kamiizumi, Sodegaura, Chiba 299-0293, Japan*

Received 31 July 2004; received in revised form 18 December 2004; accepted 13 January 2005
Available online 13 June 2005

Abstract

$Y_3Al_5O_{12}:Ce^{3+}$ (YAG:Ce^{3+}) nanophosphor powder was synthesized by glycothermal method, where a reaction between aluminum isopropoxide and acetates of yttrium and cerium(III) was induced in 1,4-butylene glycol in autoclave. According to X-ray diffraction profiles, YAG crystal structure was formed after glycothermal treatment at 300 °C for more than 1 h. The aggregation of the primary particles of ~10 nm diameter was confirmed by TEM observation and dynamic light scattering. The intensity of photoluminescence (PL) due to 5d → 4f transition of Ce^{3+} increased with increasing the aging time at 300 °C during glycothermal treatment. The inductively coupled plasma atomic emission spectroscopy revealed that the atomic ratio of Ce/(Y + Ce) remained unchanged irrespective of the aging time at 300 °C. Therefore, this suggests that prolonged aging promotes the homogeneous incorporation of Ce^{3+} into the interior of particle. Based on the characterization by thermal analysis and infrared absorption spectroscopy, the coordination of 1,4-butylene glycol and acetate on the surface of YAG:Ce^{3+} nanophosphors possibly plays a significant role in the PL enhancement.

Keywords: Phosphors; Nanofabrications; Luminescence; Nuclear resonance

1. Introduction

Ce^{3+}-doped yttrium aluminum garnet ($Y_3Al_5O_{12}$), abbreviated as YAG:Ce^{3+}, can convert from blue light to yellowish green light. This optical function is useful for potential applications such as solid-state light-emitting devices. YAG:Ce^{3+} phosphor is produced by conventional solid-state reaction at 1100–1400 °C [1,2]. Lower temperature syntheses, such as spray-pyrolysis [3,4], co-precipitation [5,6], sol–gel processing [2,7–11] and hydrothermal method [12,13] have been reported.

For the optical conversion application, a nanosize phosphor is useful for reducing the optical scattering loss. Nanoparticles have higher surface to volume ratio as compared with bulk. A surface site acts as a luminescent killer. It is, therefore, necessary to passivate the surface defects of nanophosphor with a surface modifier. For the purpose of preparing nanophosphors modified with organic species, we focused on solvothermal method. High temperature (350–600 °C) and high pressure (70–175 MPa) are needed to produce single phase YAG by hydrothermal method [12,13]. Inoue et al. developed glycothermal synthesis which is a kind of solvothermal synthesis by using glycols as solvents [14]. They reported the formation of single phase YAG from aluminum compounds and yttrium acetate in 1,4-butylene glycol (1,4-BG) at the temperatures ranging from 280 to 300 °C under autogeneous pressure [15,16]. Here we report photoluminescent (PL) properties of YAG:Ce^{3+} nanophosphor prepared by glycothermal method. This is the first report that glycothermal method enables us to incorporate a luminescent center into YAG nanoparticles without post heat treatment at high temperature.

* Corresponding author. Tel.: +81 45 566 1554; fax: +81 45 566 1551.
E-mail address: isobe@applc.keio.ac.jp (T. Isobe).

0925-8388/$ – see front matter © 2005 Elsevier B.V. All rights reserved.
doi:10.1016/j.jallcom.2005.01.066

2. Experimental

Aluminum isopropoxide (12.50 mmol) and yttrium(III) acetate tetrahydrate (7.425 mmol), cerium(III) acetate monohydrate (0.075 mmol) at Ce/(Y + Ce) = 1.0 at.% were suspended in 1,4-BG (52.8 mL) in a glass inner vessel. This vessel was placed in a 120 mL autoclave (Taiatsu Techno Corp., TVS-120-N2). Then, 1,4-BG (10.2 mL) was poured in the gap between the autoclave wall and the vessel. The autoclave was heated to 300 °C at a rate of 3.1 °C/min with stirring at 300 rpm and aged at 300 °C for $0.5\,h \leq t_{ag} \leq 4\,h$, where t_{ag} is the aging time. The autogeneous pressure gradually increased during autoclave treatment to reach 5.5 MPa at the end of aging for $t_{ag} = 4\,h$. After cooling to room temperature, ethanol was added to the colloidal solution. After centrifugating at 10^4 rpm for 10 min and washing by ethanol repeatedly three times, the precipitate was dried at 50 °C for 1 day to obtain the powder.

Crystalline phases were identified by X-ray diffractometry (XRD, Rigaku Rint 2200), using Cu Kα radiation. The particle morphology and the microstructure were observed by field emission transmission electron microscopy (TEM, Hitachi, H-800). The particle size distribution was measured by dynamic light scattering (DLS, Malvern HPPS). Photoluminescence (PL) and its excitation (PLE) spectra were measured by a JASCO FP-6500 spectrophotofluorometer, where the excitation wavelength of 460 nm was used. After dissolving the sample in an acidic aqueous solution, the concentrations of Ce, Y and Al were determined by inductively coupled plasma atomic emission spectroscopy (ICP-AES, Seiko instruments SPS-1500VR). Solid-state ^{27}Al NMR experiments were performed with a Bruker ARX-400 spectrometer operating in a static field of 9.39 T using magic angle spinning (MAS) technique, where a zirconia rotor was spun at 10 kHz. The single pulse excitation (SPE) – MAS ^{27}Al NMR spectra were measured by a single $\pi/2$ pulse of width of 2 μs with high power proton decoupling pulse. The $^{1}H \rightarrow {}^{27}Al$ cross-polarization (CP) – MAS ^{27}Al NMR spectra were measured by a single $\pi/2$ pulse of width of 4 μs with high power proton decoupling pulse, where the contact time was 500 μs. The Al chemical shift was referenced to the external standard of $Al(H_2O)_6^{3+}$. Thermogravimetry and differential thermal analysis (TG-DTA, Mac Science 2020) was carried out in an air flow (200 mL/min) at a heating rate of 10 °C /min. Fourier transform infrared (FT-IR) spectra were measured by Rio-Rad FTS175 spectrometer, using KBr disk method.

3. Results

As shown in XRD profiles (Fig. 1), a single phase of crystalline YAG was formed after autoclave treatment at 300 °C for $t_{ag} \geq 1\,h$, whereas an unidentified intermediate phase was observed at $t_{ag} = 0.5\,h$. According to TEM observation (Fig. 2), the primary particles of the samples aged at 300 °C for $t_{ag} \geq 1\,h$ were spherical in shape and their mean diameter was ca. 10 nm irrespective of aging time. The primary particle is composed of one single crystal domain, as confirmed by lattice images (see inset in Fig. 2). The size of their coalescent particles observed by TEM is close to the mean particle size, ca. 50 nm, measured by DLS.

The ^{27}Al NMR peaks were observed at 0.6, 50 and 65 ppm in the SPE-MAS spectrum of the sample aged at 300 °C for $t_{ag} = 4\,h$, whereas the peak at 3.5 ppm was observed in the

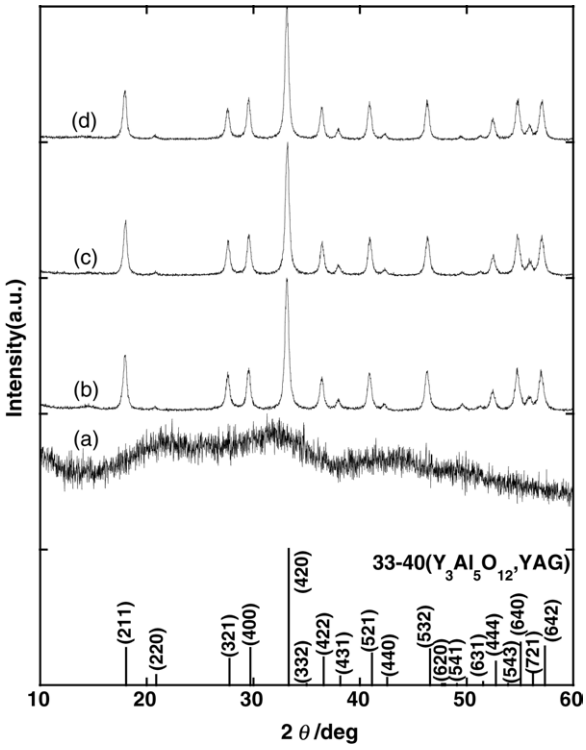

Fig. 1. XRD profiles of the samples prepared by glycothermal method and JCPDS data (no. 33–40) of YAG. Aging time at 300 °C: (a) 0.5 h, (b) 1 h, (c) 2 h and (d) 4 h.

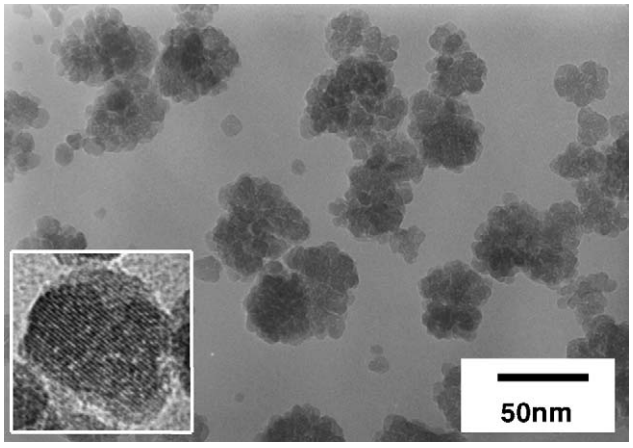

Fig. 2. TEM micrograph of the sample prepared by glycothermal method at 300 °C for $t_{ag} = 4\,h$. The inset is the lattice image.

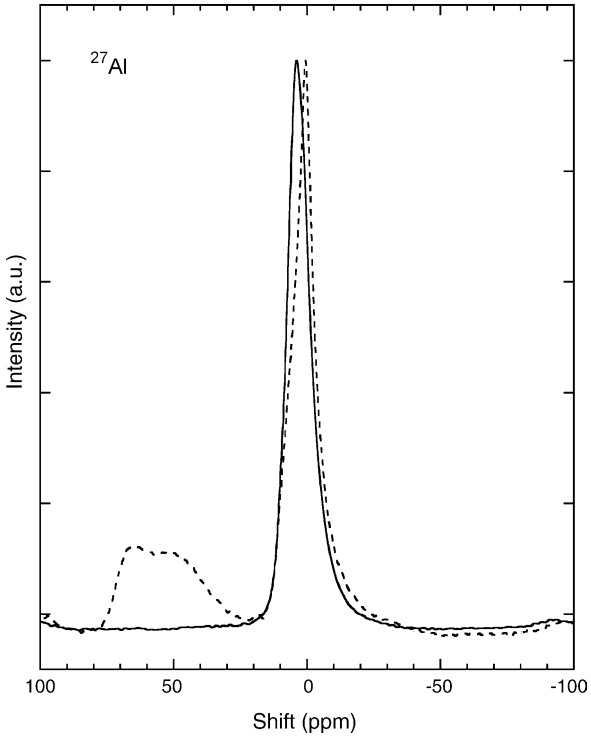

Fig. 3. Solid-state ^{27}Al MAS NMR spectra of the sample prepared by glycothermal method at 300 °C for t_{ag} =4 h. Broken line: SPE; solid line: CP.

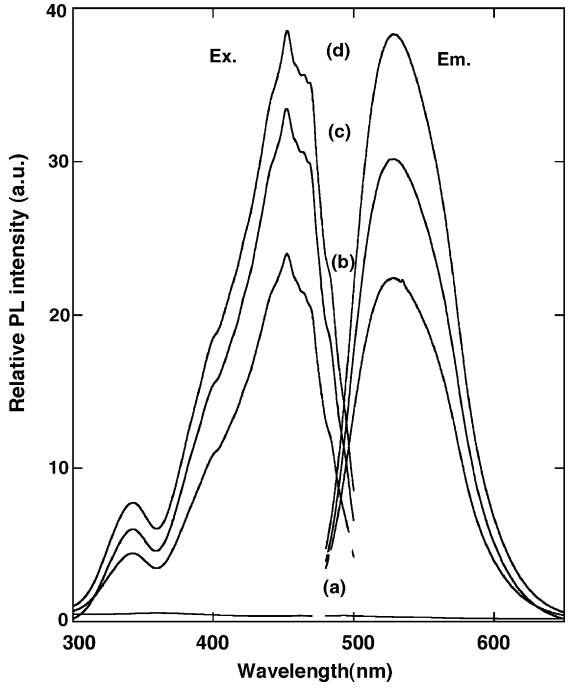

Fig. 4. PLE and PL spectra of the samples prepared by glycothermal method. Aging time at 300 °C: (a) 0.5 h, (b) 1 h, (c) 2 h and (d) 4 h.

CP-MAS spectrum, as shown in Fig. 3. Each peak at 0 and 3.5 ppm is assigned to the six-fold coordination for Al, and the peaks at 50 and 70 ppm are assigned to the four-fold coordination. The integral intensity of four-fold coordination relative to that of six-fold coordination in the SPE-MAS ^{27}Al NMR spectrum was 0.484, being smaller than 3/2 for the bulk [17]. All the Al sites are observed in the SPE-MAS spectrum, while the Al sites near the surface, i.e. near protons of organic species adsorbed on the surface are observed in the CP-MAS spectrum. Therefore, we can conclude that the four-fold coordination does not exist near the surface of YAG:Ce^{3+} nanophosphor.

Fig. 4 shows PLE and PL spectra of samples with different aging times. The asymmetric PL spectrum peaking at 530 nm is assigned to the 5d ($^2A_{1g}$) → 4f ($^2F_{5/2}$ and $^2F_{7/2}$) transitions of Ce^{3+}, since Ce^{3+} with a $4f^1$ electron configuration has two ground states of $^2F_{5/2}$ and $^2F_{7/2}$ because of the spin–orbit interaction. The PL intensity increased with increasing t_{ag}. According to elementary analysis by ICP-AES, the Ce/(Ce + Y) atomic percent, 0.95 ± 0.05 at.%, remained unchanged irrespective of the aging time.

The FT-IR peaks corresponding to the symmetric and asymmetric stretching modes of COO^- are observed for the sample aged for t_{ag} = 4 h. This indicates the adsorption of carboxyl groups in acetate salts of starting materials as well as OH groups in solvents used for synthesizing and washing. When the sample prepared by glycothermal method at 300 °C for t_{ag} = 4 h was heated to 1000 °C at 10 °C/min in air flow (200 mL/min), the PL intensity decreased by a factor of ca. 1/8. According to TG-DTA profile, the heating temperature is enough high to burn out all organic species adsorbed on nanoparticles.

4. Discussion

The results in this work verify that glycothermal method enables us to incorporate luminescent center of Ce^{3+} into well-crystallized YAG nanoparticles without post heat treatment. The PL enhancement from t_{ag} = 0.5 to 1 h is attributed to the crystallization because of the reduction of the emission killers associated with amorphous. By taking the ionic radii of Y^{3+}, Al^{3+} and Ce^{3+} into consideration [18], Ce^{3+} ions are substituted for Y^{3+} ions. The Ce/(Ce + Y) atomic ratio remained unchanged for samples with different aging times. Therefore, the increase in the PL intensity of YAG:Ce^{3+} nanophosphors with increasing t_{ag} could be explained by the following factors: (i) the actual Ce content in YAG particles, (ii) the valence states of Ce, i.e. the atomic ratio of $Ce^{3+}/(Ce^{3+} + Ce^{4+})$, (iii) the homogeneity of Ce^{3+} and (iv) the coordination states around Ce^{3+}.

We used cerium(III) acetate as a starting material. However, the oxidation of Ce^{3+} to Ce^{4+} during and after glycothermal reaction might occur on a surface site because of the adsorption of oxygen molecules [19]. If Ce^{3+} ions are localized in the near-surface and/or distributed inhomogeneously in individual particles, the concentration quenching

possibly occur. Prolonged aging promotes the homogeneous incorporation of Ce^{3+} into the interior of each particle. This decreases the concentration quenching to increase the PL intensity. At the same time, the migration of Ce^{3+} into the interior by aging prevents Ce^{3+} from interacting with adsorbed oxygen molecules on the surface, resulting in the reduction from Ce^{4+} to Ce^{3+}. This also contributes to the increase in the PL intensity. The surface site of nanoparticles is different from the interior site of nanoparticles from the viewpoints of number and symmetry of coordination around Ce^{3+}. The above-mentioned localization of Ce^{3+} ions (eight-fold coordination) near the surface and/or nanosizing of YAG:Ce^{3+} particles appears to affect the coordination for Al^{3+}, resulting in no existence of four-fold coordination for Al near the surface. Further work will be needed to understand the correlation of four factors (i)–(iv).

The organic species are decomposed by heating the YAG:Ce^{3+} nanophosphors to 1000 °C, resulting in decreasing the PL intensity. This is entirely opposite to the effect of heat treatment for the conventional methods on the PL enhancement. This result suggests that the organic species on the surface possibly plays a significant role in the passivation of surface luminescent killers and the prevention of oxidation of Ce^{3+} to Ce^{4+}. This is consistent with the above-mentioned localization of Ce^{3+} near the surface.

5. Conclusion

Glycothermal reaction of aluminum isoproxide and acetates of yttrium and cerium(III) in 1,4-butylene glycol can incorporate the luminescent center of Ce^{3+} into YAG without post heat treatment to produce well-crystallized YAG:Ce^{3+} nanophosphor of 10 nm in diameter. The surface modification, i.e. the adsorption of YAG:Ce^{3+} nanoparticles with 1,4-butylene glycol and acetates plays a significant role in the PL enhancement.

References

[1] X. Guo, K. Sakurai, Jpn. J. Appl. Phys. 39 (2000) 1230.
[2] C.H. Lu, H.C. Hong, R. Jagannathan, J. Mater. Chem. 12 (2002) 2525.
[3] S.D. Parukuttyamma, J. Margolis, H. Liu, C.P. Grey, S. Sampath, H. Herman, J.B. Parise, J. Am. Ceram. Soc. 84 (2001) 1906.
[4] Y.H. Zhou, J. Lin, M. Yu, S.M. Han, S.B. Wang, H.J. Zhang, Mater. Res. Bull. 38 (2003) 1289.
[5] Y. Murayama, S. Shiratori, Trans. Mater. Res. Soc. Jpn. 27 (2002) 791.
[6] J.G. Li, T. Ikegami, J.H. Lee, T. Mori, J. Mater. Res. 15 (2000) 2375.
[7] C.H. Lu, R. Jagannathan, Appl. Phys. Lett. 80 (2002) 3608.
[8] Q. Li, L. Gao, D. Yan, Mater. Chem. Phys. 64 (2000) 41.
[9] G. Gowda, J. Mater. Sci. Lett. 5 (1986) 1029.
[10] S.K. Ruan, J.G. Zhou, A.M. Zhong, J.F. Duan, X.B. Yang, M.Z. Su, J. Alloys Compd. 275–277 (1998) 72.
[11] M. Veith, S. Mathur, A. Kareiva, M. Jilavi, M. Zimmer, V. Huch, J. Mater. Chem. 9 (1999) 3069.
[12] Y. Hakuta, K. Seino, H. Ura, T. Adschiri, H. Takizawa, K. Arai, J. Mater. Chem. 9 (1999) 2671.
[13] B.V. Mill', Sov. Phys. Crystallogr. 12 (1967) 137.
[14] M. Inoue, H. Kominami, T. Inui, J. Am. Ceram. Soc. 73 (1990) 1100.
[15] M. Inoue, H. Otsu, H. Kominami, T. Inui, J. Am. Ceram. Soc. 74 (1991) 1452.
[16] M. Inoue, H. Otsu, H. Kominami, T. Inui, J. Alloys Compd. 226 (1995) 146.
[17] C. Landron, S. Lefloch, M. Gervais, J.P. Coutures, D. Bazin, Phys. Stat. Sol. B 196 (1996) 25.
[18] R.D. Shannon, Acta Cryst. A32 (1976) 751.
[19] A. Martínez-Arias, M. Fernández-García, V. Ballesteros, L.N. Salamanca, J.C. Conesa, C. Oteroa, J. Soria, Langmuir 15 (1999) 4796.